

# The effect of ultrasonic rolling on the fatigue performance of laser-welded TC4 titanium alloy joints

Cong Jiahui (✉ [congjiahui2011@163.com](mailto:congjiahui2011@163.com))

Shenyang Aerospace University

Gao Jiayuan

Shenyang Aerospace University

Zhou Song

Shenyang Aerospace University

Zhang Zhichao

Shenyang Aerospace University

Wang Jiahao

Shenyang Aerospace University

Wang Naijing

Shenyang Aerospace University

---

## Research Article

**Keywords:** TC4 titanium alloy, fatigue, mechanical properties, ultrasonic rolling

**Posted Date:** May 29th, 2023

**DOI:** <https://doi.org/10.21203/rs.3.rs-2958929/v1>

**License:** © ⓘ This work is licensed under a Creative Commons Attribution 4.0 International License.

[Read Full License](#)

**Additional Declarations:** No competing interests reported.

---

## **The effect of ultrasonic rolling on the fatigue performance of laser-welded TC4 titanium alloy joints**

Cong Jiahui<sup>1</sup>; Gao Jiayuan<sup>1</sup>; Zhou Song<sup>1</sup>; Zhang Zhichao<sup>1</sup>; Wang Jiahao<sup>1</sup>; Wang Naijing<sup>1</sup>.

<sup>1</sup>School of Mechatronics Engineering Shenyang Aerospace University, Shenyang 110136, China;

**Corresponding author: Cong Jiahui Tel.:8602489724538.**

**E-mail address: congjiahui2011@163.com**

**Present/permanent address: School of Mechanical & Electrical Engineering**

**Cong Jiahui E-mail address: congjiahui2011@163.com**

**Gao Jiayuan E-mail address: gaojiayuannb@163.com**

**Zhou Song E-mail address: zhousong23@163.com**

**Zhang Zhichao E-mail address: zzhichao1101@163.com**

**Wang Jiahao E-mail address: 731321083@qq.com**

**Wang Naijing E-mail address: 1285144340@qq.com**

### **Author contributions:**

**Gao Jiayuan: conceive research; perform the experiments; conceptualization; validation; formal analysis; data curation; writing—original draft preparation; writing—review and editing; visualization. Cong Jiahui: supervision; project administration; supervision; funding acquisition; investigation; resources. Zhou Song: conceptualization; methodology; validation. Zhang Zhichao: check the manuscript. Wang Jiahao and Wang Naijing: Measure; record.**

### **Declaration of Competing Interest**

The authors declare that they have no known competing financial interests or personal relationships that could have appeared to influence the work reported in this paper.

### **Acknowledgements**

This work was financially supported by the National Natural Science Foundation of China (grant number 52105157); Liaoning Provincial Education Department ( grant number JYT2020037).

### **Abstract:**

In order to improve the fatigue performance of TC4 titanium alloy laser welded joints, ultrasonic rolling treatment was adopted in this study, and different passes of rolling process were used. The research results show that the ultrasonic rolling treatment significantly improves the fatigue limit and fatigue life of the weldment. At room temperature, the fatigue strength of the weldment increases by 2.04% to 4.58%, and the corrosion fatigue life increases by 1.71 to 3.05 times. This study also deeply analyzed the

significant effects of ultrasonic rolling treatment on surface morphology, microstructure, surface residual stress and microhardness to reveal its strengthening mechanism. It was found that the ultrasonic rolling treatment shifted the crack initiation point to the subsurface and formed a hard layer with high residual stress on the surface by applying significant static pressure input and multiple treatments. This change makes the fatigue stripes narrower and denser. Compared with the traditional weld surface treatment method, ultrasonic rolling treatment significantly improves the surface quality and fatigue performance of TC4 titanium alloy laser welded joints.

**Keywords:** TC4 titanium alloy; fatigue; mechanical properties; ultrasonic rolling.

## 1 Introduction

TC4 alloy is widely used in various fields such as aerospace, shipbuilding, mechanical engineering, and vehicle engineering due to its excellent characteristics such as low density, welding performance, corrosion resistance, and toughness. During use, most titanium alloys are subjected to alternating loads, so the high-cycle fatigue life of titanium alloy structural components is very sensitive to stress concentration, especially in welded fatigue components where there are varying sizes of stress concentration in the weld area [1]. Liangbi Li et al. [2] research has shown that residual stress from welding has a significant impact on vibration fatigue life, and due to the thermal effects during welding, there are certain fatigue weaknesses in the heat-affected zone and weld area. However, laser welding technology has been widely used in aerospace material welding due to its advantages such as good heat source concentration, small heat-affected zone, and high efficiency, but it is still difficult to avoid the existence of welding defects [3].

During laser welding of TC4 titanium alloy, the fatigue fracture of the welded joint is mainly related to the microstructure and surface morphology [4]. However, defects such as undercut, cracks, and pores often occur during the welding process, which seriously affect the mechanical and corrosion resistance properties of the welded joint [5-9]. These defects cause stress concentration on the surface and near-surface, thereby forming crack initiations. These defects are prone to form fatigue cracks under cyclic loading, which in turn affects the fatigue life of titanium alloy laser-welded joints[10-13]. Therefore, it is necessary to find an effective method to enhance the strength and corrosion resistance of the welded joint. Surface strengthening techniques that have been widely applied include ultrasonic rolling, laser cladding, ultrasonic shot peening, and laser shock processing [14-17]. In particular, ultrasonic rolling strengthening

---

technology, due to its high standardization, low cost, and high processing efficiency, has been widely used in the aerospace manufacturing industry [18-19].

In recent years, ultrasonic rolling technology has been widely used in the field of surface strengthening of materials, which can enhance the strength and hardness of materials by changing the crystal structure and plastic deformation of the material surface [20]. Through ultrasonic rolling processing of TC4 alloy, a large surface plastic deformation and residual compressive stress can be obtained, effectively improving the strength and hardness of the weld joint, and reducing the defects of the weld seam[21-22]. In addition, ultrasonic rolling can also refine the surface grains of the material, improve its surface morphology and mechanical properties, and thus improve the material's corrosion resistance and wear resistance [23-26]. Zhiwei Pang et al. [27] studied the influence of ultrasonic rolling spindle speed on the surface integrity and fatigue performance of TC4, and the results showed that ultrasonic rolling refined the surface grains of TC4 and produced residual compressive stress. The lowest roughness of 0.049 $\mu\text{m}$  can be obtained at a speed of 200rpm, and the thickness of the strengthening layer can reach about 180-200 $\mu\text{m}$ . Ultrasonic rolling surface strengthening technology is a new surface nanotechnology, which is an ultrasonic rolling tool used to process the workpiece under normal temperature, making the surface organization of the workpiece undergo work hardening, which can introduce residual compressive stress to a great extent [28-29]. Dongbo Wu et al. [30] proposed a low plasticity ultrasonic rolling process to improve the surface micro morphology and residual stress of NNS blades. Feng Wang et al. [31] established a three-dimensional finite element model based on ABAQUS to simulate ultrasonic rolling and optimize the process parameters for improving the residual stress of TC4 alloy thin plates. The results showed that when the static pressure, amplitude, and time were 1100N, 10 $\mu\text{m}$ , and 0.065s, respectively, a higher residual stress can be obtained, which is beneficial to the improvement of fatigue life.

Although ultrasonic rolling has been widely applied in many fields, its research in laser welding strengthening is relatively limited. Therefore, this study conducted experimental research on the ultrasonic rolling technology applied to the flat welding joint of TC4 laser welding. The experimental results show that ultrasonic rolling technology can effectively reduce the biting defects in the welding seam area, reduce surface roughness, improve the fatigue strength, corrosion resistance, and wear resistance of the welding joint, and improve the surface hardness of the material. This indicates that ultrasonic rolling will also become an important development trend for the strengthening of laser welding

joint flatness in the future. Therefore, as a new surface strengthening technology, ultrasonic rolling has broad application prospects. In future research, the strengthening mechanism of ultrasonic rolling on laser welding can be further explored, and the process parameters of ultrasonic rolling can be optimized for different welding materials and welding methods to further improve its strengthening effect and application scope.

This study aims to analyze the mechanism of ultrasonic rolling strengthening. Surface morphology, microstructure, surface residual stress, and microhardness analysis were conducted on TC4 laser-welded joint specimens after ultrasonic rolling for 1, 3, and 5 passes. In addition, room temperature fatigue and corrosion fatigue experiments were performed on the specimens treated with different ultrasonic rolling passes, analyzing their fatigue strength, fatigue life, and fracture morphology, and comprehensively studying the effect of ultrasonic rolling on the fatigue performance of TC4 laser-welded joints. This study will help to deepen the understanding of the mechanism of ultrasonic rolling strengthening of welded joints, guide the optimization of ultrasonic rolling technology, and improve the mechanical properties and durability of welded joints.

## 2 Experimental Procedure

### 2.1 Materials

In this experiment, TC4 titanium alloy with a thickness of 2mm was selected as the material. The chemical composition (wt%) of TC4 alloy is shown in Table 1. Before laser welding, the surface of the plate was cleaned and treated to remove impurities and oil stains, and then washed and dried. IPG YLS-4000-S2T laser and MH24 welding robot were used for laser welding, and the parameters were set according to Table 2. After welding, the plate was cut into fatigue specimens and corrosion fatigue specimens by wire cutting, as shown in Figure 1(c)and(d). To avoid stress concentration caused by wire cutting, the side of the specimen was polished to a certain extent, especially the side of the weld seam.

**Table 1 Chemical composition of the TC4 titanium alloy (wt%)**

Al	V	Fe	C	N	H	O	Ti
6.02	3.79	0.03	0.05	0.04	0.013	0.065	Bal

**Table 2 Laser welding parameters**

Laser power	Welding speed	Gas flow rate	Beam spot size
-------------	---------------	---------------	----------------

---

P/W	v/(mm.s-1)	(l/min)	TEMmn/ mm
3000	2	10-12	1.5

---

## 2.2 Ultrasonic Rolling Processing

In this study, ultrasonic rolling strengthening treatment was carried out on the welding specimens. The ultrasonic rolling device, consisting of a CNC milling machine and an ultrasonic rolling head, as shown in Figure 1(a) and (b), was used to perform double-sided strengthening treatment on the welding surface of the specimens with ultrasonic rolling parameters of a static pressure of 500N, an amplitude of 10 $\mu$ m, frequency of 20 kHz, moving speed of 2 m/min, and a step length of 0.1mm. To fully strengthen the entire specimen, the ultrasonic rolling treatment should cover the weld seam zone, the heat-affected zone, and the parent material zone. The specimen needs to be placed in the corresponding clamping mold, and the strengthened area should cover the entire welded joint. During the rolling process, it is necessary to ensure that the original weld toe is completely processed into a smooth and continuous plane. To increase the smoothness of the rolling ball, lubricating oil can be moderately dripped onto the ultrasonic rolling ball. The welding specimens were divided into four groups in this study. The first group was the control group, with no ultrasonic rolling treatment performed, and the specimen was labeled as "original". The second group of specimens underwent one ultrasonic rolling treatment, and the specimen was labeled as "N1". The third group of specimens underwent three ultrasonic rolling treatments, and the specimen was labeled as "N3". The fourth group of specimens underwent five ultrasonic rolling treatments, and the specimen was labeled as "N5".

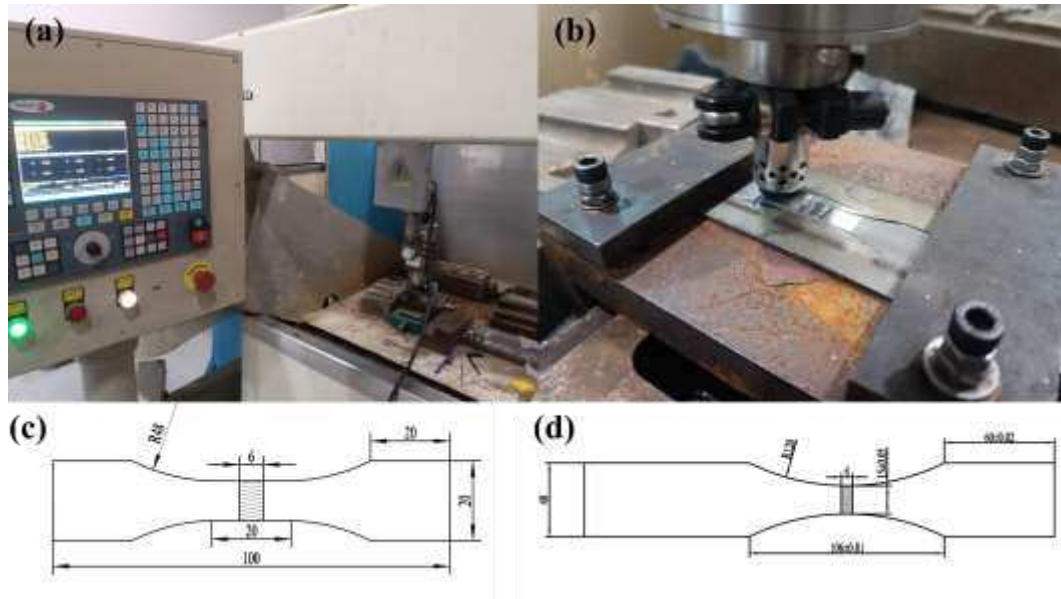


**Figure 1 (a) Ultrasonic rolling device (b) Ultrasonic rolling head;(c) Dimensional drawing of the fatigue specimen;(d) Dimensional drawing of the corrosion fatigue specimen**

### 2.3 Microstructure and Microhardness Measurement

In the study, the samples before and after strengthening were embedded, polished, and etched using an etchant for approximately 10 seconds. Afterwards, they were rinsed with water and dried using a blow dryer. The Olympus GX51 optical microscope was used to observe the macro morphology and microstructure of the welded joints before and after ultrasonic rolling strengthening. The Huayin HVS-1000A digital micro-Vickers hardness tester was used to test the surface hardness at intervals of 0.25mm with a load of 100g for 15 seconds, and the depth was tested at intervals of 0.01mm.

### 2.4 Surface Morphology and Surface Roughness Measurement

In this study, the surface morphology of the welding specimens before and after ultrasonic rolling strengthening was observed using an Olympus GX51 optical microscope. Prior to the experiment, the samples were immersed in acetone and then subjected to ultrasonic cleaning using an ultrasonic cleaner. After drying with a blower, the samples were directly placed on the operating table of the Olympus GX51 optical microscope, and the surface of the samples was observed and measured using a 50x objective lens. The high point of the weld and the surface of the parent material next to the weld were observed and photographed in front of the lens. Surface roughness was measured using a Sivaka precision roughness meter, with the center of the weld as the reference point and the measuring interval controlled at 2mm on both sides of the weld. The measuring length at each position was 5mm, and the roughness of the welding

---

joint was measured.

## **2.5 Residual Stress Measurement**

The  $\mu$ -X360 residual stress detector was used to measure the axial residual stress of TC4 titanium alloy laser-welded surface. The measurement conditions were  $\text{CoK}\alpha$  target material, diffraction plane of (3,1,1), and measurement angle of  $23.8^\circ$ . For residual stress measurement, the Young's modulus of the material was 110 Gpa, Poisson's ratio was 0.34, and the lattice constants  $a$  and  $c$  were 1.5873 and 4.6826, respectively. During the measurement, the front side of the weld was the main focus, and the measurement was performed vertically to both sides of the weld from the middle of the weld, with a measurement interval controlled at 3mm.

## **2.6 Mechanical and Fatigue Performance Measurement**

The QBG-100 high-frequency fatigue testing machine was used to perform fatigue testing on the laser-welded specimens before and after strengthening. The tests were conducted in air, using a sinusoidal load type for tensile loading with a stress ratio of  $R=0.1$  and an average loading frequency of approximately 95 Hz. Four sets of specimens were tested.

In addition, the Langjie 100 fatigue testing machine was used to perform corrosion fatigue testing, as shown in Figure 2. The experiment was conducted in a simulated seawater environment, with the test sample completely immersed in an organic glass container, and the simulated environment consisting of a 3.5% NaCl solution. The cyclic stress ratio was  $R=0.1$ , the tensile stress was 520 MPa, and the loading frequency was 10 Hz. The specimens were subjected to corrosion fatigue testing. During the test, the welding joint of the specimen must be completely immersed in the corrosive solution. The corrosive solution should enter the test box through the lower water inlet and flow out from the upper outlet to ensure a stable flow rate of the corrosive solution and a specified liquid level. Conduct three corrosion fatigue tests on each of the four types of specimens: original, N1, N3, and N5, and calculate the average value of the test results.

In the room temperature fatigue and corrosion fatigue tests, the specimens were continuously loaded until they fractured. After fracture, the specimens were cleaned using ultrasound and wiped with acetone, then dried with a blower. Finally, the NOVANANOSEM450 scanning electron microscope (SEM) was used to observe the high-frequency fatigue fracture and corrosion fatigue fracture before and after ultrasonic rolling treatment.



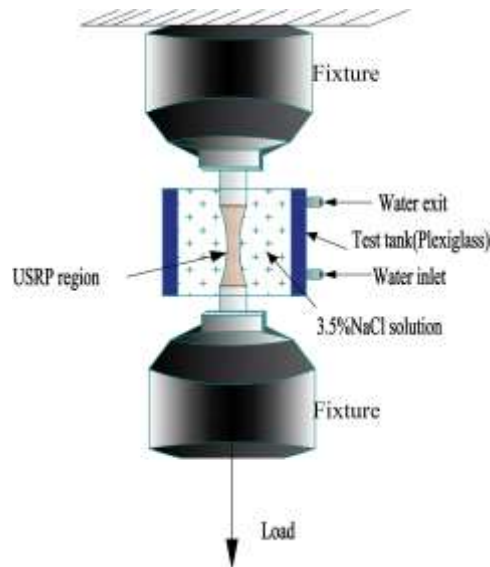


**Figure 2 Schematic diagram of the corrosion fatigue test setup**

### 3 Test Results and Analysis

#### 3.1 Microstructure and Microhardness of Cross-sections

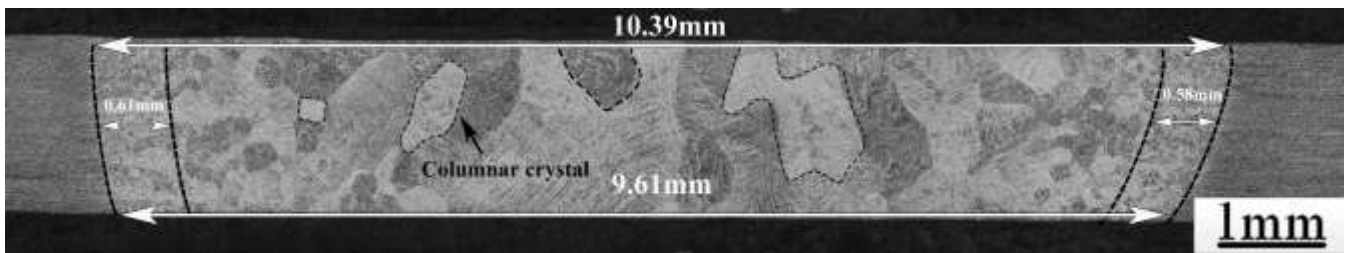
Figure 3 shows the macrostructure of the TC4 laser-welded joint. It can be seen that the laser welding is fully penetrated and the upper and lower surfaces are relatively flat. The width of the upper part of the weld is about 10.39 mm, while the width of the lower part is about 9.61 mm. The width of the weld is relatively uniform, and the laser penetration is good. According to the morphology of the microstructure, the welded joint can be roughly divided into three parts: the base metal region (BM), the heat-affected zone (HAZ), and the weld zone (HZ). The microstructure of the weld zone mainly contains coarse columnar grains, and some of the coarse columnar grains at the bottom are connected into pieces. When transitioning from the center of the weld to the base metal on both sides, the coarse grains gradually become smaller and denser. Some columnar grains are sharp-edged, which become finer and gradually transition to the base metal region in the heat-affected zone.

Figure 4(a-h) shows the changes in cross-sectional microstructure morphology under different ultrasonic rolling passes. It can be clearly seen that the microstructure after ultrasonic rolling treatment has a certain plastic deformation layer. With the increase of rolling passes, the thickness of the plastic deformation layer gradually increases, thus giving the sample a certain strengthening effect. In Figure 3(a), the microstructure of the original welding joint parent metal area is composed of equiaxed  $\alpha$  phase and  $\beta$  phase, and the surface is basically consistent with the inside. However, in Figures 3(b), (c), and (d), with the increase of ultrasonic rolling passes, the plastic deformation layer gradually thickens after more

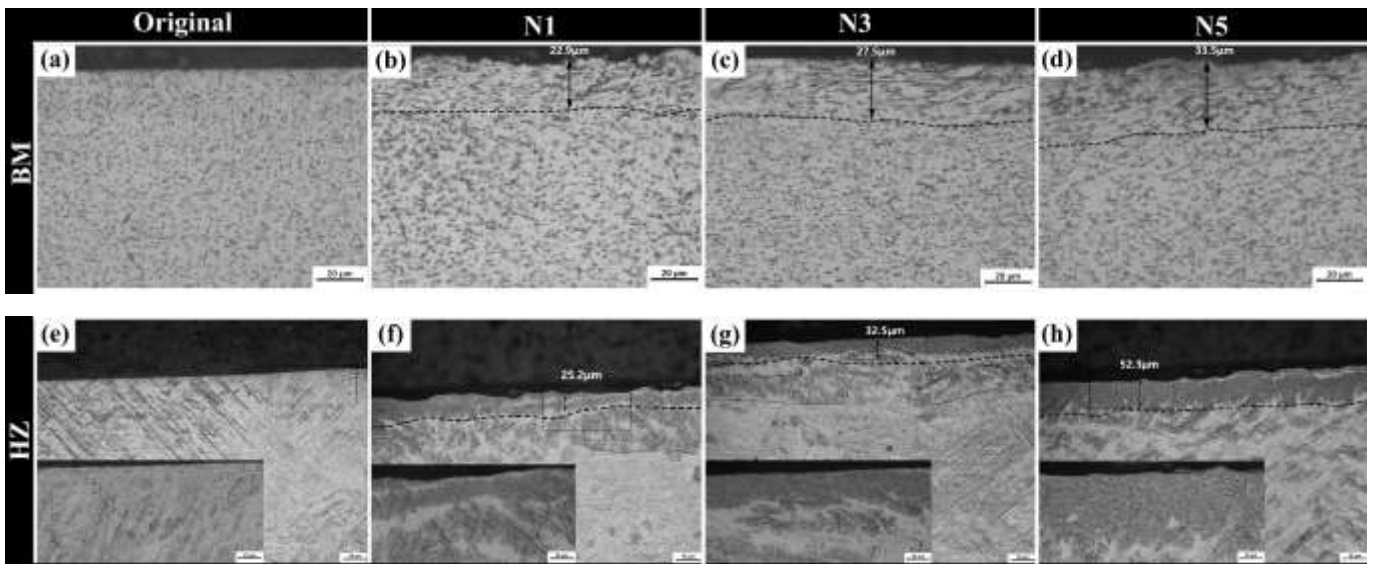
---

severe impact and rolling. After one, three, and five passes of ultrasonic rolling treatment, the thickness of the plastic deformation layer in the parent metal area is approximately 19.1  $\mu\text{m}$ , 21.3  $\mu\text{m}$ , and 25.4  $\mu\text{m}$ , respectively. After ultrasonic rolling treatment, the surface grains become more compact and wave-like elongated ridges appear, which are caused by the dislocations and flow between grains. At the same time, through the observation of the plastic deformation layer, we can see that the surface is relatively uneven after one pass of ultrasonic rolling treatment, which is caused by the impact pits, pressure ridges, and pressure valleys in some areas due to continuous impact and rolling of ultrasonic rolling. After three passes of ultrasonic rolling treatment, the surface is relatively flat and the wave-like fine ridges of the plastic deformation layer are more uniform. However, after five passes of ultrasonic rolling treatment, although the thickness of the plastic deformation layer is significantly increased, several interlayer pores appear on the surface, which is due to the relaxation effect of excessive ultrasonic rolling on the plastic deformation layer of the surface. But the wave-like fine ridges inside become denser and more compact.

It is evident from Figures 4(e-h) that compared to the original base metal region, the surface of the weld zone will form a dense plastic deformation layer after ultrasonic rolling treatment, with a thickness of about 25.2  $\mu\text{m}$ , 32.5  $\mu\text{m}$ , and 52.3  $\mu\text{m}$  (results for specimens N1, N3, and N5). This is because the weld zone has higher hardness and brittleness compared to the base metal. During the ultrasonic rolling process, the surface of the weld zone is slightly crushed and then some of the surface layer is rolled, which can further deepen the etching effect and form a thicker plastic deformation layer on the surface. Compared with the weld zone, the base metal is relatively soft and has some elasticity. After ultrasonic rolling treatment, the surface of the base metal will form a wavy pattern, and although there is no obvious change in the near surface, the grain boundaries have become denser, which is important for the strengthening of the specimen. In addition, ultrasonic rolling treatment can gradually refine the grain size of the specimen surface, thereby forming a dense strengthening layer on the surface of the weld zone, which can effectively inhibit the initiation of cracks. At the same time, ultrasonic rolling can make the weld zone smoother and the stress distribution more uniform, effectively reducing the degree of stress concentration. As the number of rolling passes increases, the thickness of the plastic deformation layer will gradually increase, and the surface smoothness will also be greatly improved. It should be noted that there are no clear boundaries between the plastic deformation layer of the base material and the substrate, as well as between the plastic deformation layer of the weld and the substrate. The plastic deformation zone is often thicker than the visible plastic deformation layer, and measurement results may have unavoidable errors.



**Figure 3 Macrostructure of the welded joint**

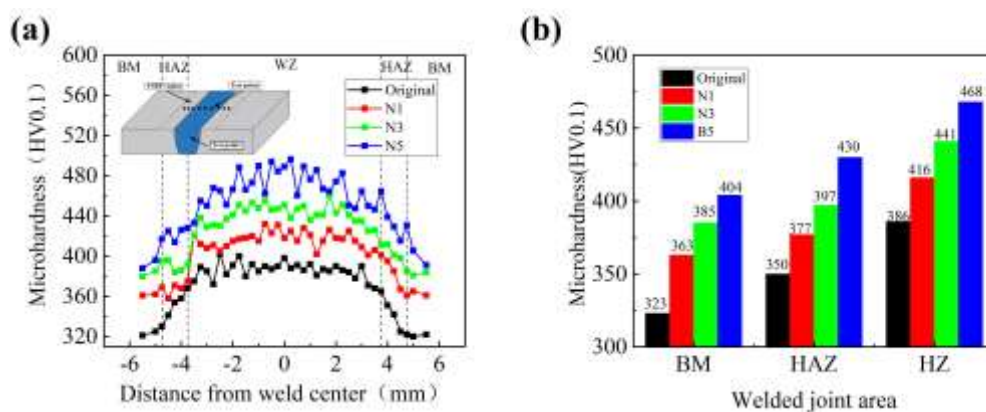


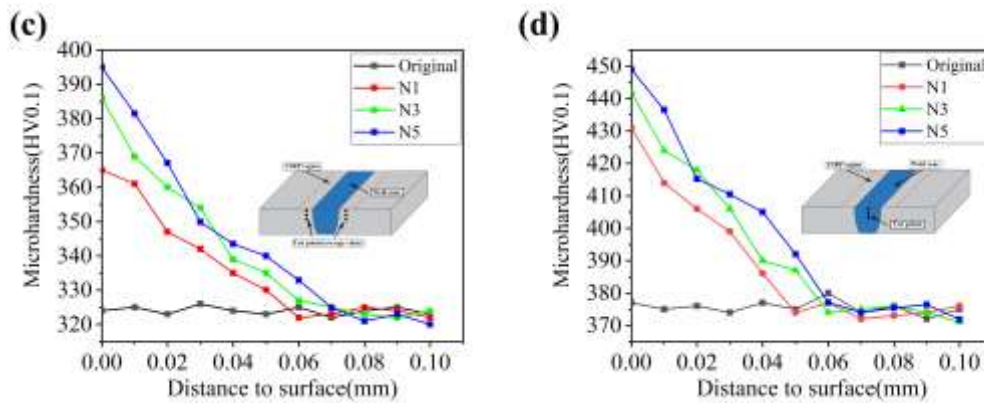
**Figure 4 Microstructure of the welded joint before and after ultrasonic rolling with different processing passes.**

Figure 5 shows a comparison of microhardness between specimens after ultrasonic rolling and the original specimens. It can be observed that the microhardness of the specimens after ultrasonic rolling is generally higher than that of the original specimens, and the microhardness gradually increases with the number of rolling passes. This indicates that ultrasonic rolling can effectively improve the surface hardness of the specimens. Specifically, Figure 5(a) shows the distribution of microhardness of the original weld joint. The microhardness gradually increases from the base metal to the weld zone. The significant increase in microhardness in the weld zone is mainly due to the formation of a large number of needle-shaped martensite inside the material caused by high temperature and rapid cooling. In addition, ultrasonic rolling makes the surface grain structure more compact, improves surface density, and thereby increases microhardness. Figure 5(b) shows that after ultrasonic rolling with N1, N3, and N5 passes, the average microhardness of the base metal, heat-affected zone, and weld zone all increase to varying degrees. After N1 ultrasonic rolling, the microhardness of the base metal, heat-affected zone, and weld

zone increased by 12.4%, 7.7%, and 7.8%, respectively, compared to the original specimens. After N3 ultrasonic rolling, the microhardness of the base metal, heat-affected zone, and weld zone increased by 19.2%, 13.4%, and 14.2%, respectively, compared to the original specimens. After N5 ultrasonic rolling, the microhardness of the base metal, heat-affected zone, and weld zone increased by 25.1%, 22.9%, and 21.2%, respectively, compared to the original specimens. This indicates that ultrasonic rolling can significantly improve the surface hardness, wear resistance, and corrosion resistance of the weld joint.

From Figure 5(c) and (d), it can be seen that the depth of influence of microhardness on the samples after ultrasonic rolling is different in the base metal area compared to the weld area. In the base metal area, the depth of influence of microhardness is deeper than that in the weld area, which is related to the high original hardness in the weld area. With an increase in the number of rolling passes, the depth of influence in the base metal area gradually increases, reaching a maximum of 0.065mm after five treatments. In the weld area, the depth of influence of microhardness increases slightly with an increase in the number of rolling passes, with a maximum depth of 0.06mm, but lower than that in the base metal area. It should be noted that due to the unclear boundary of microhardness within the samples, there may be some deviation in the measurement results. Overall, with an increase in the number of rolling passes, the degree of work hardening increases, the grain size becomes finer, and the dislocation density gradually increases.





**Figure 5 Microhardness of specimens before and after ultrasonic rolling with different numbers of passes:(a) Surface hardness; (b) Average hardness;(c) Hardness along depth in base metal; (d) Hardness along depth in weld metal**

### 3.2 Surface Residual Stress

Figure 6 shows the distribution of surface residual stress on TC4 specimens after different numbers of ultrasonic rolling treatments. It can be seen from the Figure that there is residual tensile stress at the center of the original welding seam on the surface, which gradually decreases along both sides of the seam, and the residual stress in the base material area remains at around 0 MPa, while the residual tensile stress in the center of the welding seam reaches about 158 MPa. As residual tensile stress is harmful to the welded joint, it is necessary to reduce this stress level. The reason why the original welding seam has such high residual stress is mainly due to uneven expansion during high-temperature welding and uneven contraction during cooling [32].

After undergoing ultrasonic rolling treatment for different numbers of times, the surface residual stress of the specimens was significantly reduced, and the tensile residual stress in the center of the weld was transformed into compressive residual stress, gradually decreasing with the distance from the center of the weld. The average residual stress of the weld of specimens N1, N3, and N5 decreased to about -414 MPa, -527 MPa, and -660 MPa, respectively, indicating that multiple ultrasonic rolling treatments can effectively increase the compressive residual stress on the surface of the specimens. In addition, although the compressive residual stress in the central weld zone was slightly lower than that in the base metal zone, the residual stress distribution was relatively uniform, which is beneficial to delaying the formation of cracks.

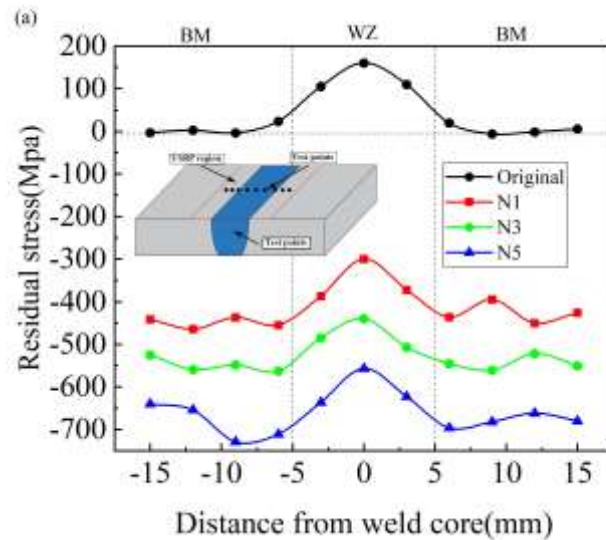


**Figure 6 Surface residual stress of welded joints before and after different ultrasonic rolling processing passes**

### 3.3 Surface Morphology and Surface Roughness

Figure 7 Through visual observation, it can be found that the height of the weld seam of the original laser welding joint is small and relatively flat, but there are many scratches and damages on the surface, which has a certain impact on the quality of the welding joint. However, after multiple ultrasonic rolling treatments, the surface of the welding joint becomes significantly integrated, the height of the weld seam gradually becomes flat, and the surface defects are reduced. Especially for TC4 laser welding joints, after ultrasonic rolling treatment, their surface morphology has been greatly improved, and the overall quality has been improved.

Figure 8(a) clearly shows that there are numerous cross scratches on the surface of the original base material caused by the grinding machine. After ultrasonic rolling treatment shown in Figure 8(b), most of the scratches were rolled flat, and the surface showed ultrasonic rolling ball-produced pressure ridges and pressure grooves, accompanied by a few microcracks and impact pit defects. The overall surface had a cloudy ultrasonic rolling treatment trace. Due to the precise control of the milling machine, the gaps between the pressure ridges and pressure grooves were uniform, and the height difference was not significant. After three and five passes of ultrasonic rolling treatment shown in Figures 8(c) and (d), the cloudy traces produced by ultrasonic rolling treatment were significantly reduced, and microcracks and impact pit defects were also significantly reduced. The pressure ridges and pressure grooves became shallower, and the overall surface flatness was higher.

Through Figure 8(e), it can be clearly seen that the original weld surface has a large number of cracks, which are caused by uneven distribution of welding heat and cooling. Many block-like crack defects are formed at the weld height, which will greatly affect the fatigue performance of the original specimen. At the same time, the weld height will also cause significant stress concentration at the weld toe, reducing the fatigue life of the specimen. Through Figures 8(f), (g), and (h), it can be clearly seen that after multiple ultrasonic rolling treatments, the crack defects on the weld surface are gradually integrated and flattened, the cracks are significantly reduced, and the weld height gradually becomes flatter.

In summary, after multiple ultrasonic rolling treatments, both the surface integrity of the base metal and the weld zone were significantly improved. Especially after N5 times of ultrasonic rolling treatment, the scratches and cracks in the base metal and weld zone were almost eliminated, and the surface flatness reached the optimal state.

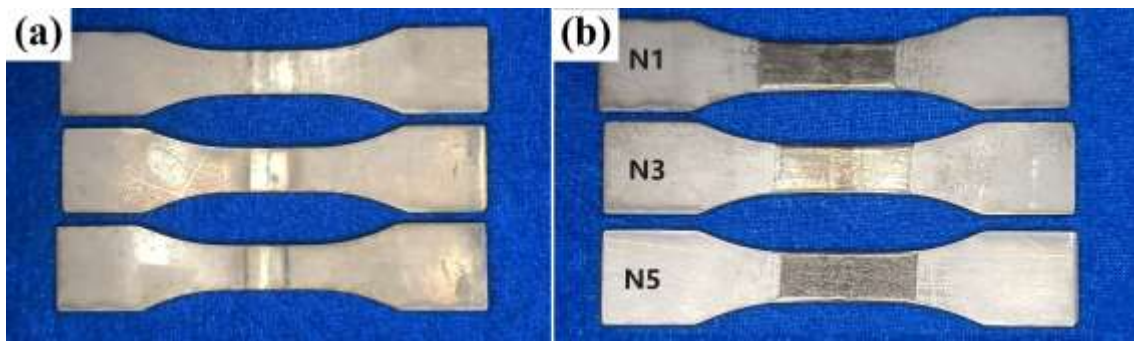
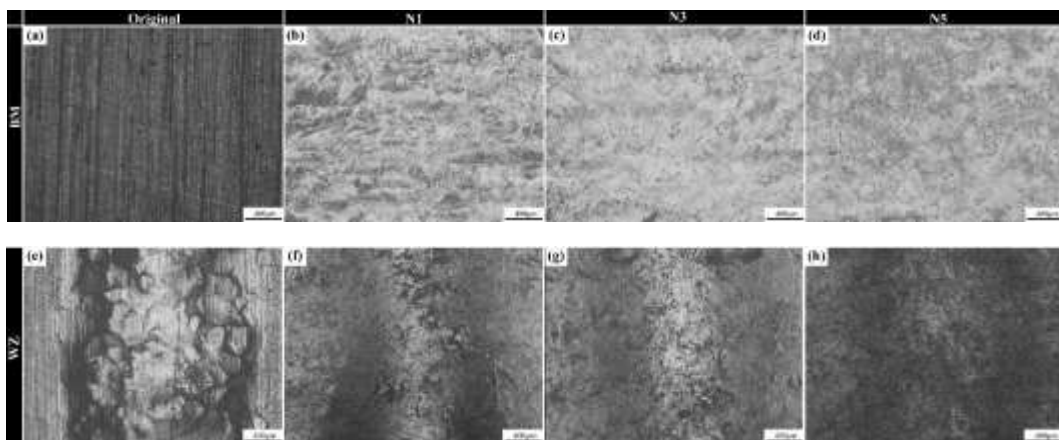
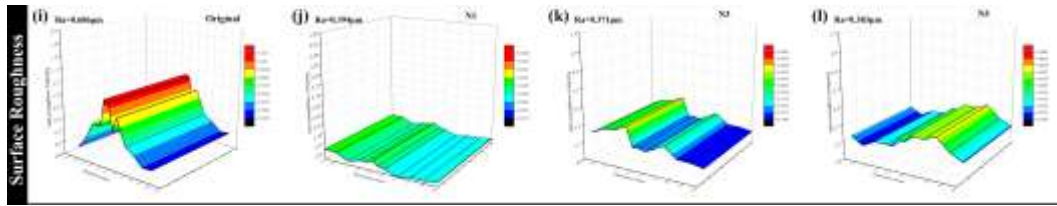


Figure 7 (a) Original specimen; (b) Specimen after ultrasonic rolling.





**Figure 8 Surface morphology of welded joints after different ultrasonic rolling processing passes.**

Figure 8 (i-l) shows the change in surface roughness of the USRP weld joint after different numbers of ultrasonic rolling processing. As shown in Figure 8(i), the surface roughness of the unprocessed weld joint is relatively high in the central area, reaching up to  $1.174\mu\text{m}$ , and gradually decreases away from the center, with an overall average surface roughness of  $0.686\mu\text{m}$ . Figure 8(j) shows that after one ultrasonic rolling processing, the overall surface of the weld joint becomes flat, and the surface roughness significantly decreases, with an average value of  $0.394\mu\text{m}$ . However, as shown in Figures 8(k) and (l), multiple ultrasonic rolling processing did not significantly improve the surface roughness of the sample, and even after five ultrasonic rolling processing, the surface roughness slightly rebounded. Therefore, the surface roughness around the weld seam basically remained unchanged after one ultrasonic rolling processing, but the overall surface roughness was lower than that of the unprocessed sample. The original sample had a large height difference at the weld seam, which would cause stress concentration, and the ultrasonic rolling processing effectively reduced the weld seam height difference and formed a smooth transition arc, thereby reducing the stress concentration effect in the weld seam area.

### 3.4 Room Temperature Fatigue Experiment

In this study, the original welding joint was subjected to multiple ultrasonic rolling processing, and fatigue tests were conducted under different stress ranges [33]. Figure 9 shows the S-N curves of the TC4 laser welding joint in the as-welded state and after different numbers of ultrasonic rolling processing. The results show that the fatigue life of the welding joint significantly increased after ultrasonic rolling processing.

By subjecting the original welded joint to multiple ultrasonic rolling treatments and conducting fatigue tests at different stress levels, the fatigue strength of the welded joint under 0.1 stress ratio and  $2 \times 10^6$  cycles was calculated using the S-N curve equation for different numbers of ultrasonic rolling treatments. According to the data in Table 3, the fatigue strength of the original welded joint was 349.47 MPa. Compared with the original welded joint, the fatigue strength of the welded joint increased by 2.04%, 3.00%, and 4.58% after one, three, and five ultrasonic rolling treatments, respectively, reaching 356.61



MPa, 359.97 MPa, and 365.48 MPa. Therefore, the fatigue strength of the welded joint can be effectively improved with increasing rolling passes. The specific reason for this phenomenon is that ultrasonic rolling treatment can refine the surface grain of the welded joint and increase the dislocation between grains. Meanwhile, it can also produce a plastic deformation layer with high hardness, reduce the height of the weld residual height, make the transition arc of the weld toe area smoother, and thus make the overall stress more uniform. In addition, ultrasonic rolling treatment can reduce surface roughness, reduce stress concentration, and inhibit the initiation and propagation of crack initiations. Multiple ultrasonic rolling treatments can also introduce residual compressive stress on the surface of the specimen, which can effectively counteract the external applied load and reduce the actual load stress.

After one ultrasonic rolling treatment, the fatigue life of the welding joint was greatly improved in all stress stages. However, the percentage increase in life under high load stress decreased after multiple treatments. In addition, the fatigue life of sample N5 was slightly lower than that of sample N3 under higher stress, indicating that multiple ultrasonic rolling treatments did not show significant advantages in the early stage of fatigue loading. This is mainly because ultrasonic rolling can greatly reduce the surface roughness of the welding joint, but after multiple ultrasonic rolling treatments, the surface roughness gradually increases after reaching saturation. When the applied load is large, the defects in the surface roughness are amplified.

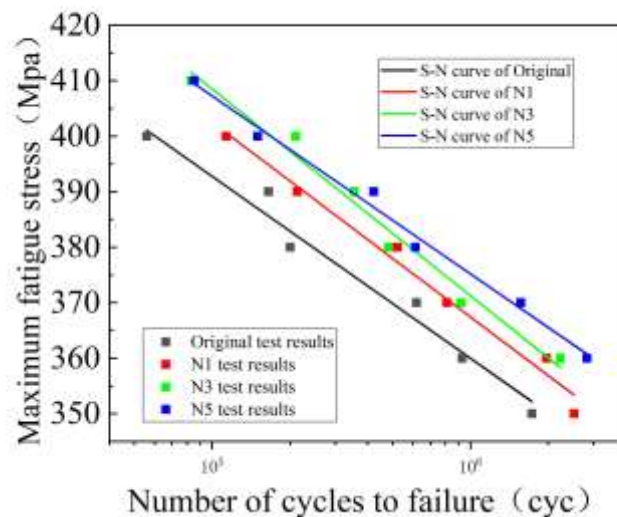


**Figure 9 S-N curve of welded joints before and after different ultrasonic rolling processing passes of passes**

**Table 3 S-N Curve Equations of Welded Joints before and after Ultrasonic Rolling with Different Numbers of Passes. (R=0.1)**

Sample	Median S-N curve equation	Characteristic S-N curve equation	$S_c$	Fatigue strength ( $2 \times 10^6$ )(MPa)	Improvement rate (%)
Original	$\lg N = 70.08 - 25.07 \lg \Delta \sigma$	$\lg N = 69.87 - 25.07 \lg \Delta \sigma$	0.091	349.47	-
N1	$\lg N = 67.95 - 24.15 \lg \Delta \sigma$	$\lg N = 67.77 - 24.15 \lg \Delta \sigma$	0.074	356.61	2.04
N3	$\lg N = 65.81 - 23.28 \lg \Delta \sigma$	$\lg N = 65.64 - 23.28 \lg \Delta \sigma$	0.073	359.97	3.00
N5	$\lg N = 76.43 - 27.36 \lg \Delta \sigma$	$\lg N = 76.30 - 27.36 \lg \Delta \sigma$	0.058	365.48	4.58

### 3.5 Corrosion Fatigue Experiment

Figure 10(a) shows the average corrosion fatigue life of laser-welded TC4 titanium alloy joints before and after different numbers of ultrasonic rolling processing cycles. It is evident that the corrosion fatigue life of the welded joint specimens is effectively improved after ultrasonic rolling processing. The fatigue life cycles of the original specimen were 35467, while those of specimens subjected to multiple ultrasonic rolling processing cycles (N1, N3, and N5) were 60587, 83312, and 108118, respectively, which are 1.71 times, 2.35 times, and 3.05 times the fatigue life of the original specimen. Therefore, with the increase in the number of ultrasonic rolling cycles, the corrosion fatigue life of the specimens gradually increases.

Under the combined effects of corrosion and fatigue, the specimen is prone to fracture due to both fatigue-induced failure and corrosion-induced cracking. Therefore, the use of ultrasonic rolling technology, as shown in Figure 10(b), can improve the corrosion fatigue life of the specimen. Ultrasonic rolling can refine the grain size inside the specimen, generate a large number of dislocations, and produce dislocation boundaries. At the same time, residual compressive stress is introduced on the surface of the specimen, causing a closing effect at the crack tip, flattening the weld toe, improving surface smoothness, and increasing the microhardness of the surface layer. The resulting dense plastic deformation layer can form a passive film on the surface, which inhibits the progress of corrosion. With the increase in the number of ultrasonic rolling passes, surface defects are gradually flattened, roughness is significantly reduced, near-surface grains are gradually refined, and the thickness of the formed plastic deformation layer also gradually increases, thereby delaying the rupture of the passive film. Therefore, ultrasonic rolling technology can effectively suppress the generation and propagation of cracks, improve the corrosion resistance, and enhance the corrosion fatigue life of the specimen.

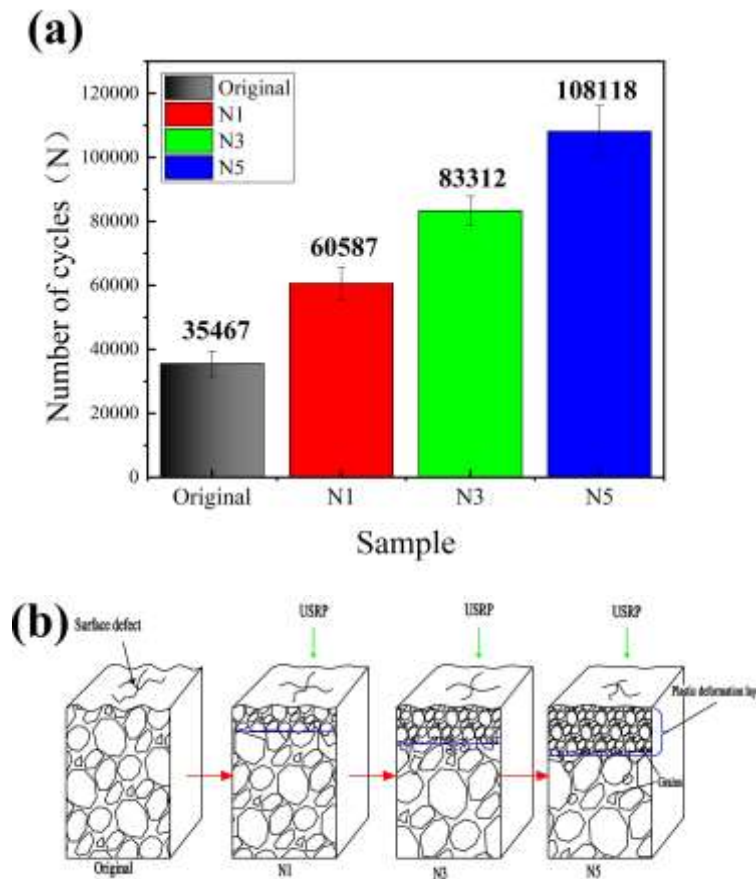


**Figure 10 (a)Average corrosion fatigue life of welded joints before and after different ultrasonic rolling passes;(b) Corrosion fatigue fracture mechanism.**

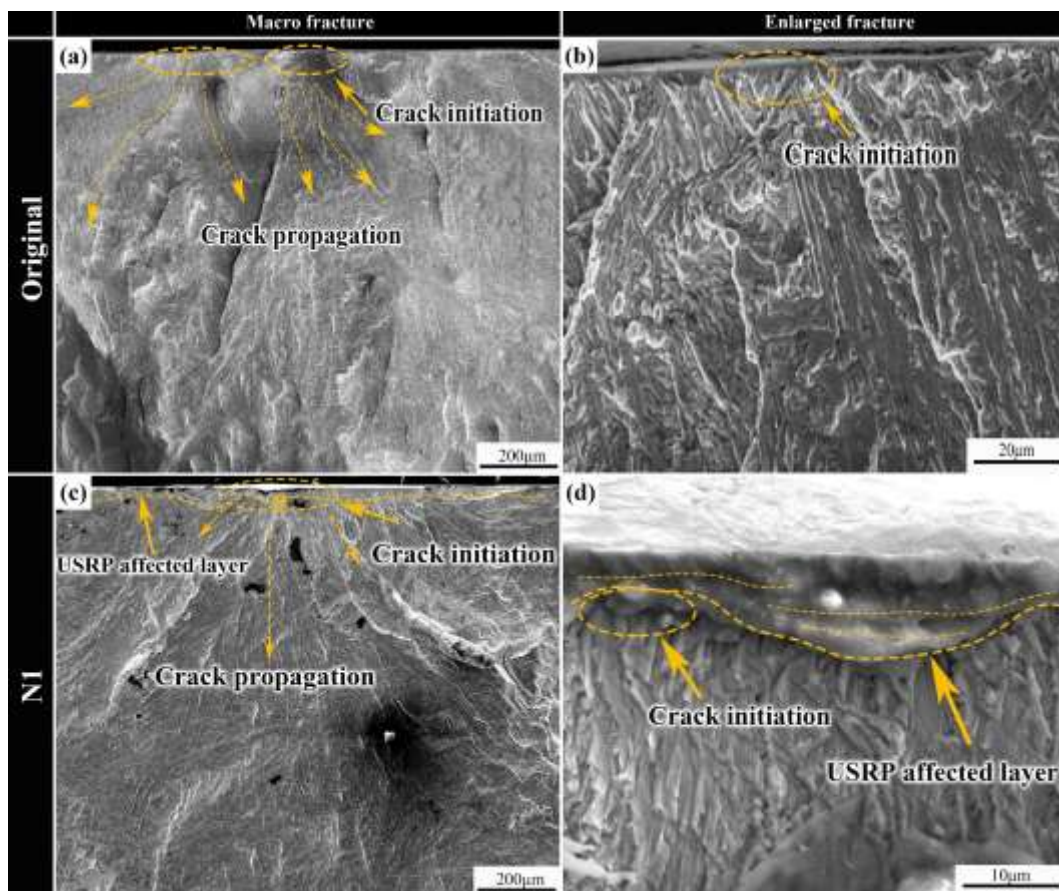
### 3.6 Analysis of Fracture Surface Morphology

The NOVANOSEM450 scanning electron microscope (SEM) was used to observe the high-frequency fatigue fracture and corrosion fatigue fracture before and after ultrasonic rolling treatment. The strengthening mechanism of ultrasonic rolling on room temperature fatigue and corrosion fatigue of TC4 titanium alloy laser welding was analyzed comprehensively.

#### 3.6.1 Room Temperature Fatigue

As shown in Figure 11, the high-frequency fatigue fracture morphology before and after ultrasonic rolling treatment and corrosion fatigue fracture were observed using the NOVANOSEM450 scanning electron microscope (SEM). The effect of ultrasonic rolling on the fatigue and corrosion fatigue of TC4 titanium alloy was thoroughly analyzed. The fatigue crack initiation of the original welded sample often appeared on the surface of the welded sample, and multiple fatigue crack initiations could occur, radiating from the crack initiation and expanding into the interior of the sample, as shown in Figures 11(a) and (b). The crack propagation path was often relatively straight. However, for the ultrasonic rolling-treated

samples, the fatigue crack initiation often appeared in the subsurface layer, as shown in Figures 11(c-h). This is because, after ultrasonic rolling treatment, a hard layer often forms on the surface of the sample, which also has high residual stress. The surface grains are nano-sized, forming a strengthening layer, which inhibits the formation of crack initiations on the surface. However, as the fatigue experiment progresses, the ability of the residual stress on the sample surface to counteract the applied load gradually decreases, causing the fatigue crack initiation to originate from the subsurface layer with weaker residual stress. With an increasing number of ultrasonic rolling treatment passes, the position where the fatigue crack initiation is initiated gradually shifts downward, and enlarged images show that the degree of grain refinement increases with an increasing number of ultrasonic rolling treatment passes near the surface. Some grains elongate into thin layers, the lattice orientation changes, and dislocations form between crystals, effectively inhibiting the initiation of crack sources. On the other hand, ultrasonic rolling reduces surface roughness and decreases surface defects, making it difficult for crack initiations to initiate on the surface.



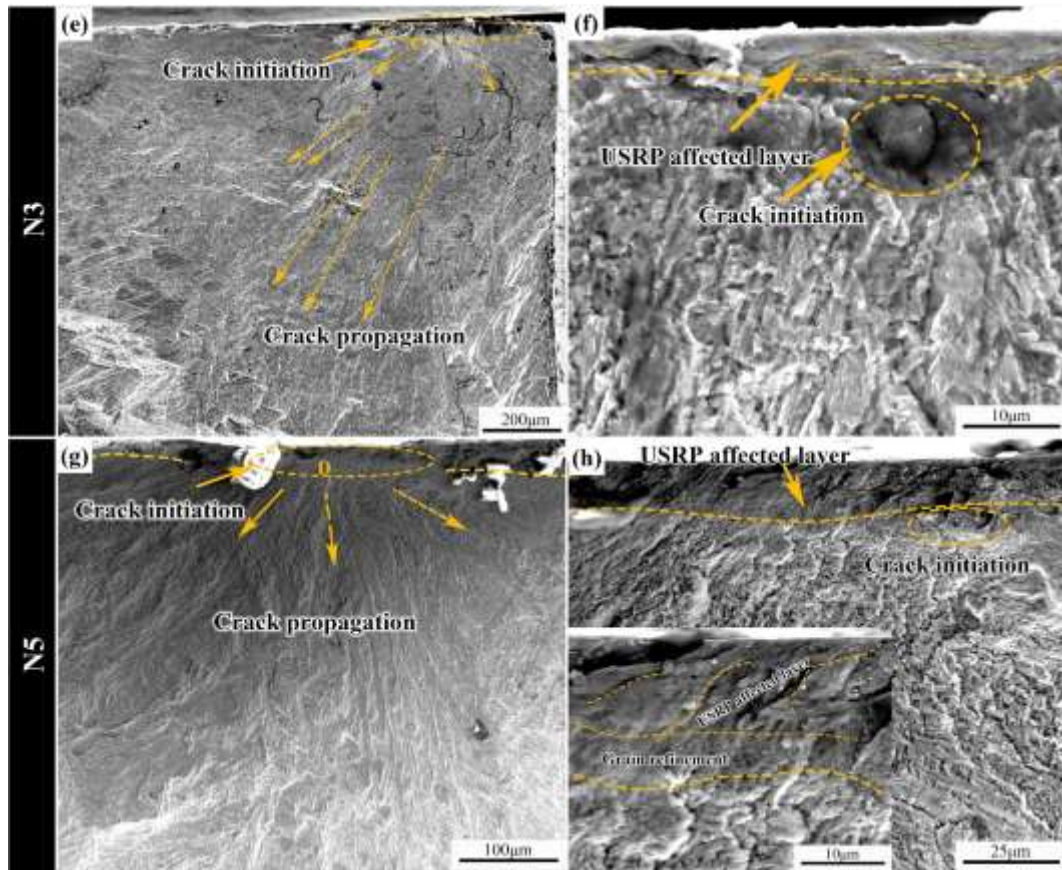


**Figure 11 Fatigue crack initiation fracture morphology of welded joints.**

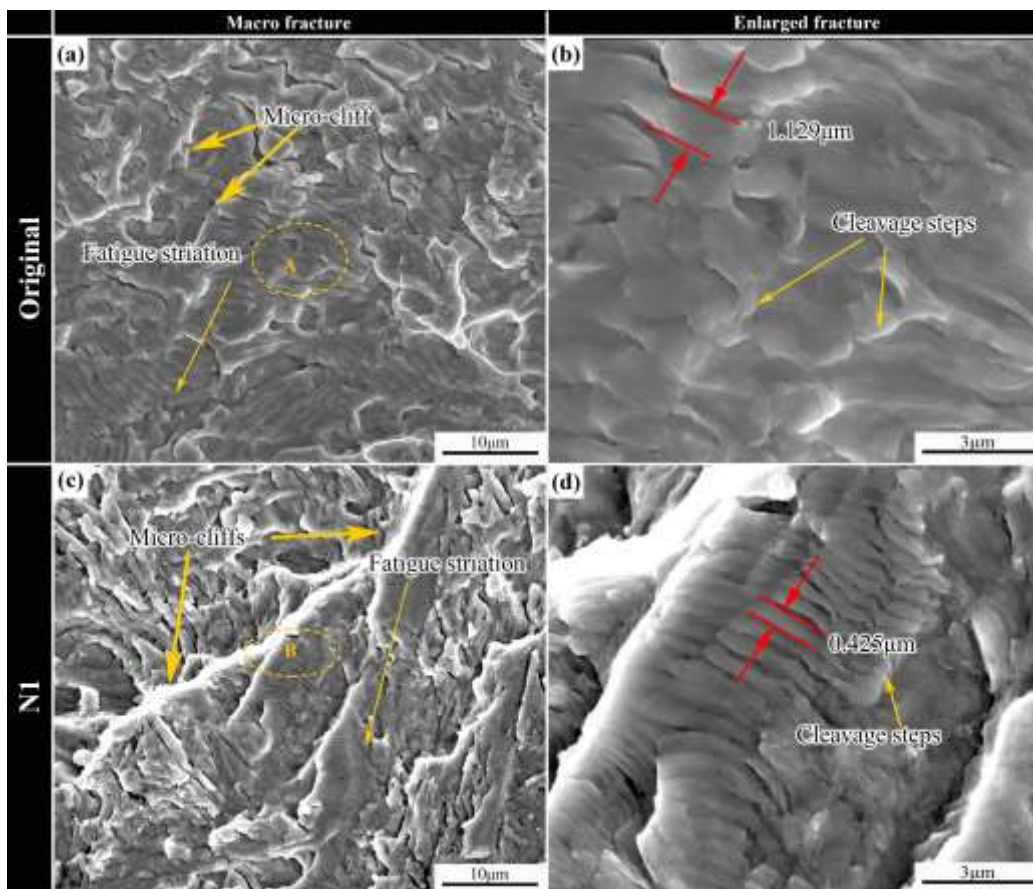
Figure 12 shows the fracture surface morphology of the crack propagation zone of specimens after different numbers of ultrasonic rolling processing passes. From Figures 12(a) and (b), it can be seen that the crack propagation band width of the original sample is wide, about  $1.129 \mu\text{m}$ . From the macroscopic morphology diagram, the entire propagation zone is relatively flat and smooth, and the propagation direction is relatively smooth without too much variation. After ultrasonic rolling processing, a large number of micro-undulations are generated in the propagation zone, causing the direction of the crack propagation path to begin to change multiple times, thereby inhibiting the continuous propagation of the crack. The density of the crack bands increases and the width narrows. By observing Figures 12(f) and (h), it can be found that some secondary cracks will be generated on the cleavage planes in the crack propagation zone. The generation of these secondary cracks will consume part of the energy of crack propagation and reduce the crack propagation rate.

In addition, it can be noted that after ultrasonic rolling, the extension region forms many cleavage steps, which are caused by the high-density dislocations and lattice distortions generated by ultrasonic rolling[6,34]. During the process of crack extension, these cleavage steps will cause the crack band to

break on the lattice planes, thereby inhibiting the extension of the crack band. This mechanism can slow down the crack propagation rate, improve th' material's toughness and ductility.

By observing Figure 12(c-h), it is evident that with an increase in the number of ultrasonic rolling passes, the density of fatigue striations gradually increases, the roughness of the extension zone surface also increases, while the width of fatigue striations gradually narrows. The fatigue striation widths of samples N1, N3, and N5 are approximately  $0.425\mu\text{m}$ ,  $0.299\mu\text{m}$ , and  $0.227\mu\text{m}$ , respectively, which are reduced by 62.4%, 73.5%, and 79.9% compared to the original sample. It is evident that ultrasonic rolling can significantly reduce the width of fatigue striations.

The above phenomenon indicates that ultrasonic rolling effectively reduces the crack propagation rate, and with an increase in the number of ultrasonic rolling passes, the ability to inhibit crack propagation gradually strengthens. This effect is attributed to the large compressive residual stress generated by ultrasonic rolling. When a fatigue crack propagates, the compressive residual stress can reduce the stress field around the crack, thereby reducing the magnitude of the stress intensity factor. At the same time, the compressive residual stress can also change the stress state and reduce the stress ratio. In addition, the micro-closure effect caused by compressive residual stress can effectively inhibit crack propagation.



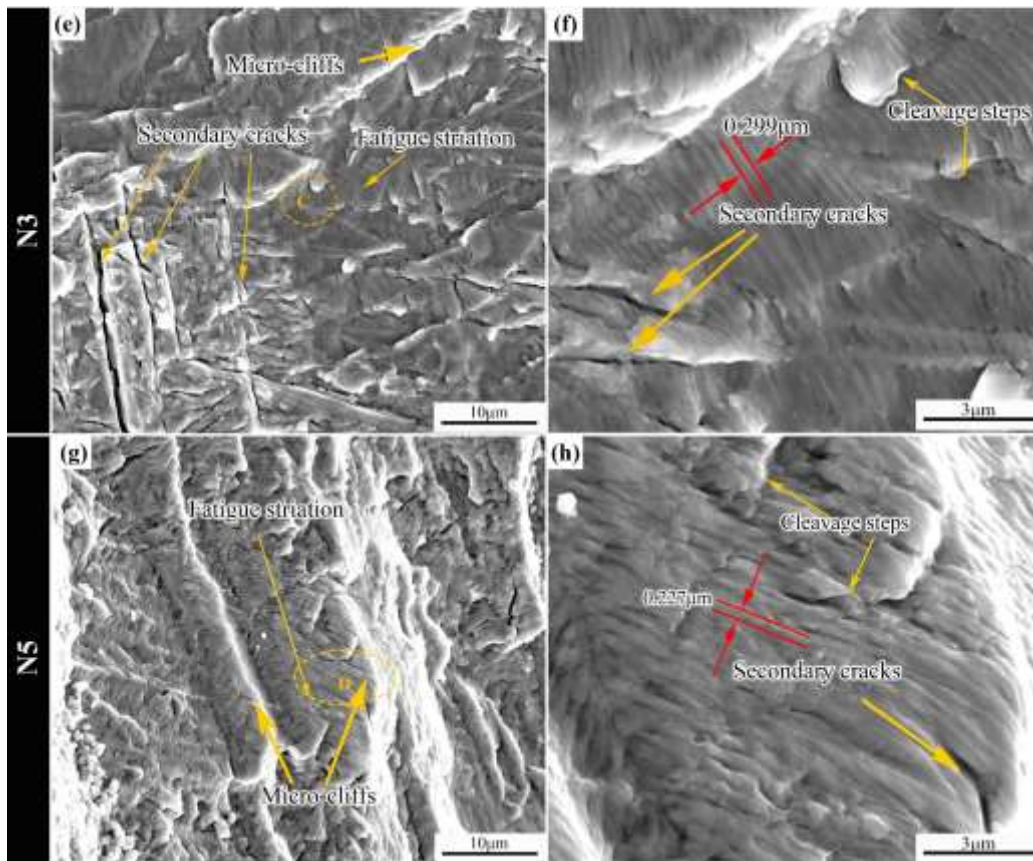


**Figure 12** Fracture surface morphology of fatigue crack propagation area.

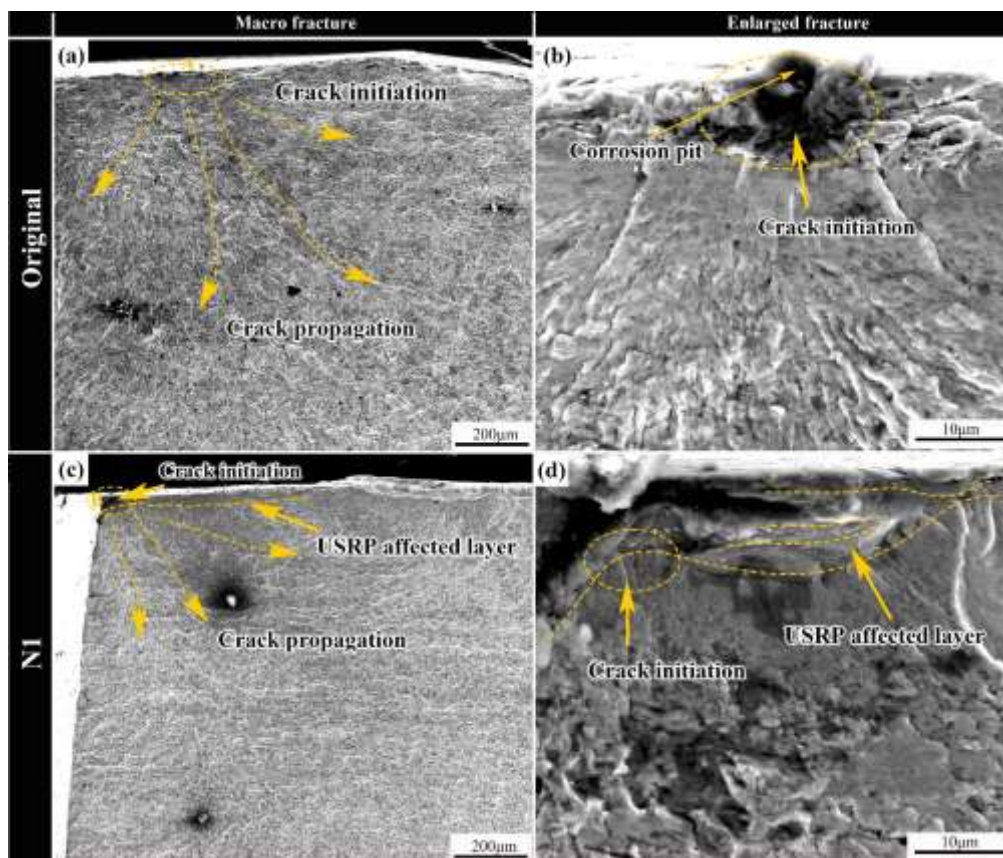
### 3.6.2 Corrosion Fatigue

Figure 13 shows the corrosion fatigue fracture surfaces before and after ultrasonic rolling at different numbers of passes. As shown in Figure 13(a), the crack propagation path of the untreated sample is relatively flat, straight, and without any obvious deflection. In the enlarged region A (Figure 13(b)), it can be seen clearly that the crack initiation site of the original sample is at the surface defect, which leads to the rapid fracture of the corrosion fatigue sample. In contrast, as shown in Figures 13(c-h), the crack propagation path of the ultrasonic-rolled sample is rugged with multiple changes. In addition, a hard layer with higher residual stress is formed on the surface, which suppresses the crack initiation at the surface layer. Therefore, the crack initiation usually occurs in the sub-surface layer with weaker residual stress. With an increase in the number of ultrasonic rolling passes, the hard layer on the surface thickens, and the crack initiation site moves downward, effectively suppressing the crack initiation.

On the other hand, the original sample is affected by corrosion, which forms small corrosion pits on the surface of the TC4 titanium alloy laser welding joint sample. These pits can cause stress concentration and become the starting point of cracks. Under external loads, the stress is concentrated around the corrosion

pits, leading to the crack initiation and propagation. In addition, the oxide layer on the titanium alloy surface affects its electrochemical characteristics, and the crack will form a corrosion concentration zone under the oxide layer. Chloride ions in the corrosion solution will gather here and trigger electrochemical reactions, which can destroy the surface of the titanium alloy. As the crack propagates, titanium will be exposed on the surface and react with the corrosive medium, forming pitting and exacerbating stress concentration, which forces the crack propagation to accelerate. Therefore, as shown in Figure 11, corrosion products usually occur at the crack initiation site.

The ultrasonic rolling technology can reduce surface roughness, improve the surface quality of the welded joint, and introduce a larger residual compressive stress in the surface layer. This process can refine grains and produce a plastic deformation layer, effectively suppressing the formation of surface corrosion defects.





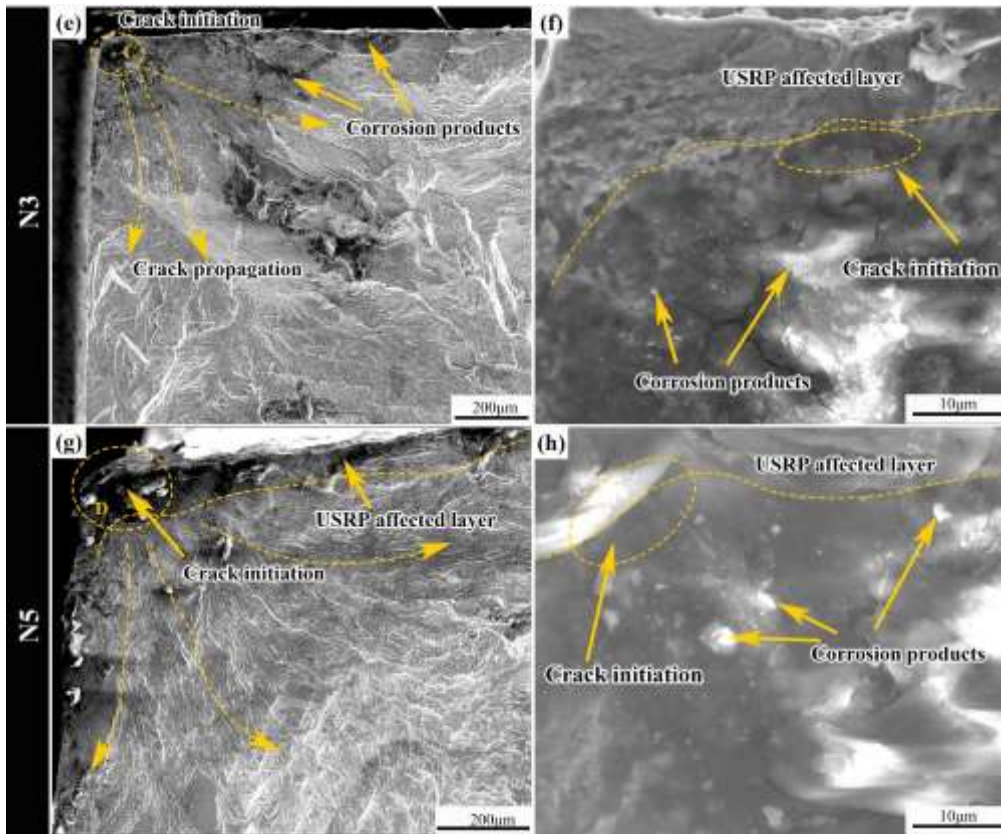


**Figure 13 Corrosion fatigue crack initiation fracture morphology of the welded joint.**

Figure 14 shows the morphologies of the corrosion fatigue striations before and after different ultrasonic rolling passes. By comparing (a) and (b) in Figure 14, it is apparent that the original specimen exhibits a smooth and wide fatigue extension path, with a striation width of up to  $1.059\ \mu\text{m}$ . In contrast, by comparing (e-h) in Figure 14, after ultrasonic rolling treatment, the extension path becomes more tortuous and erratic, with multiple changes in direction and level. The distribution of the fatigue striations also becomes disorderly, appearing as intermittent patches with an increasing number of ultrasonic rolling passes. The extension area is often affected by the corrosion medium, which generates corrosion products. Micro-cliffs and cleavage steps surround the fatigue striations, inhibiting their extension. By observing magnified images (A, B, C, and D in (b), (d), (f), and (h) of Figure 14), it can be seen that the fatigue striations become denser with an increasing number of ultrasonic rolling passes. The width of the striations gradually narrows, and secondary cracks appear. Moreover, the fatigue striation widths of specimens N1, N3, and N5 decrease by 45.2%, 57.7%, and 58.8%, respectively, compared to the original specimen. Therefore, based on the aforementioned observations, it can be inferred that ultrasonic rolling can effectively reduce the extension rate of corrosion fatigue, thus improving the fatigue life of the specimens.

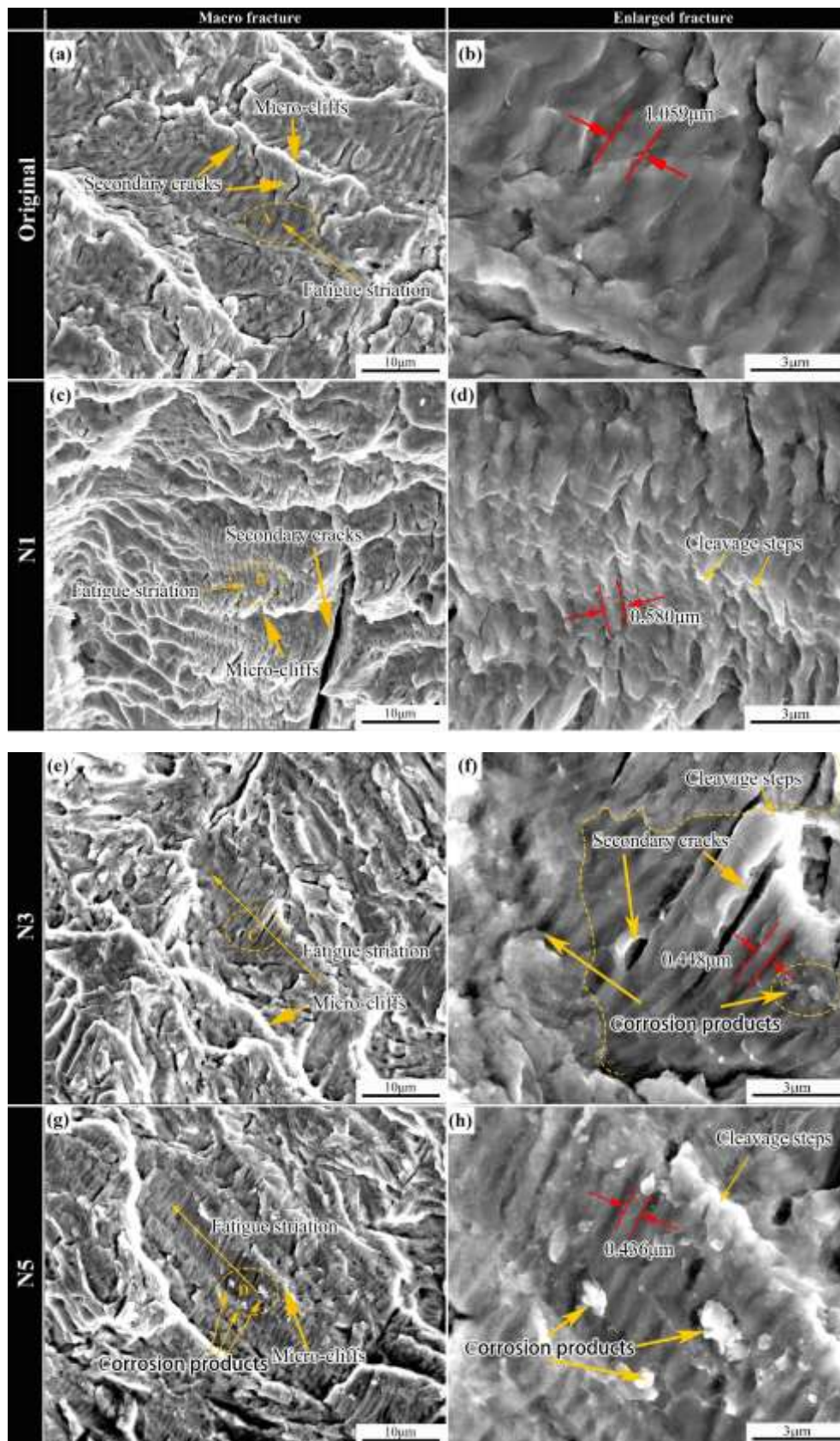


Figure 14 Morphology of corrosion fatigue propagation zone of welded joints.

#### 4. Discussion

Figure 15 illustrates the schematic diagram of the strengthening mechanism of ultrasonic rolling on the fatigue performance of TC4 titanium alloy laser welded joints. The fatigue performance of TC4 welding joints is affected by multiple factors, including surface roughness, surface residual stress, microhardness, and near-surface microstructure [35]. Through figures 15(a) and (c), it is clear that there are numerous scratches and pores, among other defects, on the surface of the original TC4 laser welding joint. Due to the welding defects, a large number of square cracks are formed on the surface of the weld bead height at the back of the weld seam, with the highest surface roughness. These surface defects will generate multiple fatigue sources under cyclic loading and corrosion, leading to a reduction in fatigue life. After multiple ultrasonic rolling treatments, the scratches, pores, and other defects on the surface of the specimen are significantly reduced, and a large number of square cracks at the weld bead height are gradually eliminated, making the surface structure more dense.

The residual stress on the surface of a specimen has a significant impact on its fatigue performance and can suppress crack propagation rate. During laser welding, residual tensile stress is often generated on the surface of the specimen, which creates a driving force from the inside out. The superimposition of residual tensile stress and external loading increases the actual load and accelerates the formation of fatigue sources, thus accelerating the crack propagation rate. After multiple ultrasonic rolling treatments, the residual stress on the surface of the specimen changes from residual tensile stress to residual compressive stress. The larger residual compressive stress has a driving force from the outside in, and when superimposed with external loading, effectively reduces the actual load. At the same time, residual compressive stress produces crack closure effects at the crack tip, reducing the stress intensity factor at the crack tip, thus effectively inhibiting crack initiation and delaying crack propagation.

From figures 15(b) to (d), it can be clearly seen that the original welded joint has a large weld bead height, a small transition radius in the weld toe area, and a large number of defects on the weld surface, which can easily cause stress concentration and lead to surface crack formation. On the fracture surface of the original specimen, the fatigue crack propagation path is single and smooth, without much obstruction, which is not conducive to improving the fatigue life of the specimen. The width of the fatigue striations in the crack propagation zone is large, and the density is low.

However, after multiple ultrasonic rolling treatments, compared to the original welded joint, the weld bead height becomes flattened and the transition radius in the weld toe area becomes larger. The near-surface

grains become fine and dense, and a large number of dislocation structures are formed between the grains. The dislocation structures between adjacent grains require more energy for fatigue crack initiation and propagation. During the ultrasonic rolling process, a large amount of plastic deformation occurs on the specimen surface, forming a hard layer with high hardness. In terms of corrosion fatigue, a passive film is formed on the specimen surface, which inhibits the formation and propagation of fatigue sources on the surface. Therefore, the fatigue source often forms below the near-surface layer, and the propagation path formed is tortuous, with many interruption points and termination lines. This is mainly due to the plastic deformation layer with a large number of dislocation structures formed by ultrasonic rolling, which extends to deeper positions. The grains have different orientations and high-density dislocation structures (dislocation lines, dislocation tangles, and dislocation walls), making the crack experience more grain boundary structures during propagation. This leads to a more chaotic and disorderly crack propagation direction, which suppresses crack propagation [17]. After multiple ultrasonic rolling treatments, the fatigue fracture zone formed a large number of tearing ridges and narrower, denser fatigue striations, as well as numerous secondary cracks between them. Tearing ridges and secondary cracks indicate that more energy has been consumed during fatigue crack growth. Large numbers of cleavage steps were formed at the edge of the fatigue striations, which can cleave the extension of fatigue striations at the lattice level and cause them to fracture and become shorter in the transverse direction, hindering the propagation of cracks.

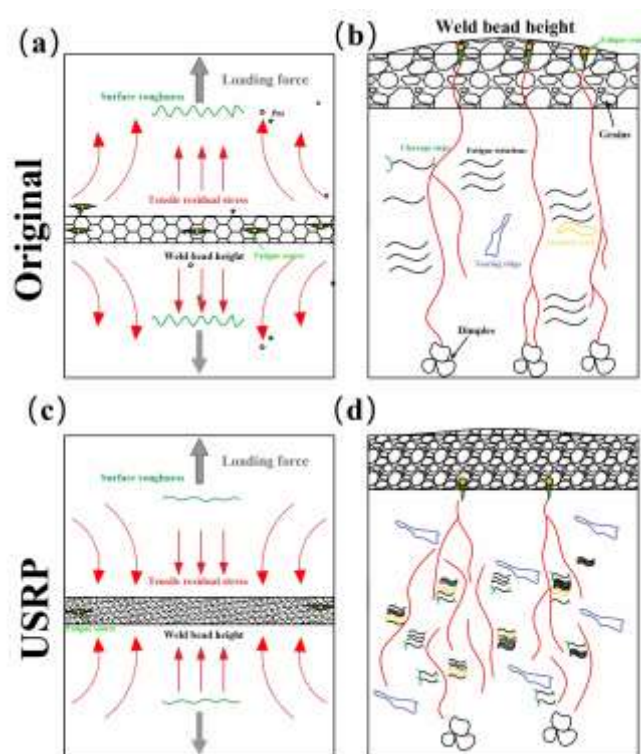


**Figure 15 Schematic diagram of the strengthening mechanism of ultrasonic rolling on the fatigue performance of TC4 titanium alloy laser welding joint.**

## **5 Conclusion**

In this study, the TC4 laser-welded joints were processed with different ultrasonic rolling numbers to achieve good surface quality and comprehensive performance. Meanwhile, the room temperature fatigue performance and corrosion fatigue performance of the samples before and after multiple treatments were greatly improved. Based on the experimental results and theoretical analysis, the following conclusions can be drawn:

1. With the increase of ultrasonic rolling processing times, the surface quality of the sample gradually improves. Among them, the N5 sample has the best surface integrity, with an average surface roughness of 0.383  $\mu\text{m}$ , an average surface residual stress value of -660 MPa, the maximum plastic deformation layer in different regions, and the highest microhardness in different regions. The average microhardness of the weld surface of the N5 sample is about 468 HV.
2. After different numbers of ultrasonic rolling treatments, the fatigue performance of the sample is significantly improved. In this study, the room temperature fatigue strength of the N1, N3, and N5 samples increased by 2.04%, 3.00%, and 4.58%, respectively, and the corrosion fatigue was 1.71 times, 2.35 times, and 3.05 times that of the original fatigue life of the sample. Ultrasonic rolling treatment has a significant improvement effect on the fatigue performance of the TC4 welding joint.
3. After multiple ultrasonic rolling treatments, the room temperature fatigue crack initiation of the TC4 laser-welded joint often moves downward to the sub-layer to form a hard layer on the surface with a larger residual stress. The crack propagation path is tortuous and there are multiple deflection phenomena. Similarly, the corrosion fatigue sample processed by multiple ultrasonic rolling treatments thickens the hard layer on the surface, moves the crack initiation downward, improves the surface quality through ultrasonic rolling, reduces the influence of the corrosive medium, and extends the growth cycle of the crack initiation.
4. As the number of treatments increases, the fatigue striations become denser and narrower, and secondary cracks appear. High-density dislocations and lattice distortions produced by the treatments cause the formation of cleavage steps, inhibiting the extension of the fatigue striations. Compared to the original sample, the width of the fatigue striations is reduced by 62.4%, 73.5%, and 79.9% (room

---

temperature fatigue) and 45.2%, 57.7%, and 58.8% (corrosion fatigue) for N1, N3, and N5, respectively.

## References

- [1] Shi X, Feng X, Teng J, Zhang K, Zhou L (2021) Effect of laser shock peening on microstructure and fatigue properties of thin-wall welded Ti-6Al-4V alloy. *Vacuum* 184: 109986.  
<https://doi.org/10.1016/j.vacuum.2020.109986>
- [2] Li L, Gu X, Sun S, Wang W, Wan Z, Qian P (2018) Effects of welding residual stresses on the vibration fatigue life of a ship's shock absorption support. *Ocean Eng* 170: 237–245.  
<https://doi.org/10.1016/j.oceaneng.2018.10.011>
- [3] Akman E, Demir A, Canel T, Sınmazçelik T (2009) Laser welding of Ti6Al4V titanium alloys. *J Mater Process Technol* 209: 3705–3713.  
<https://doi.org/10.1016/j.jmatprotec.2008.08.026>
- [4] Shui J, Chen SL, Xia TT, et al. (2022) Effect of non-equilibrium solid state phase transformation on welding temperature field during keyhole mode laser welding of Ti6Al4V alloy. *Opt Laser Technol* 145: 107461.  
<https://doi.org/10.1016/j.optlastec.2021.107461>
- [5] B. Wang, H. Peng, and Z. Chen, Microstructure and Mechanical Properties of a Laser Welded Ti–6Al–4V Titanium Alloy/FeCoNiCrMn High Entropy Alloy with a Cu Filler Layer, *J. Mater. Res. Technol* 12(2021), 1970.  
Wang B, Peng H, Chen Z. (2021) Microstructure and mechanical properties of a laser welded Ti–6Al–4V titanium alloy/FeCoNiCrMn high entropy alloy with a Cu filler layer. *J. Mater. Res. Technol* 12: 1970–1978.  
<https://doi.org/10.1016/j.jmrt.2021.04.010>
- [6] Feng X, Pan X, He W, Liu P, An Z, Zhou L. (2021) Improving high cycle fatigue performance of gas tungsten arc welded Ti6Al4V titanium alloy by warm laser shock peening. *Int J Fatigue* 149: 106270.  
<https://doi.org/10.1016/j.ijfatigue.2021.106270>
- [7] Junaaid M, Baig MN, Shamir M, Khan FN, Rehman K, Haider J. (2017) A comparative study of pulsed laser and pulsed TIG welding of Ti-5Al-2.5Sn titanium alloy sheet. *J Mater Process Technol* 2017;242: 24 – 38.  
<https://doi.org/10.1016/j.jmatprotec.2016.11.018>
- [8] Cheng H, Zhou L, Li Q, Du D, Chang B. (2021) Effect of welding parameters on spatter formation

- in full-penetration laser welding of titanium alloys. *J. Mater. Res. Technol* 2021;15: 5516 – 5525.  
<https://doi.org/10.1016/j.jmrt.2021.11.006>
- [9] Xu P, Li L, Zhang C (Sam). (2014) Microstructure characterization of laser welded Ti-6Al-4V fusion zones. *Mater Charact* 2014;87: 179 – 185.  
<https://doi.org/10.1016/j.matchar.2013.11.005>
- [10] Chen J, Li H, Liu Y, et al. (2023) Deformation behavior and microstructure characteristics of the laser-welded Ti-6Al-4V joint under variable amplitude fatigue. *Mater Charact* 2023;196: 112606.  
<https://doi.org/10.1016/j.matchar.2022.112606>
- [11] Yunlian Q, Ju D, Quan H, Liying Z.(2000) Electron beam welding, laser beam welding and gas tungsten arc welding of titanium sheet. *Mater. Sci. Eng. R Rep.: A* 2000;280: 177 – 181.  
[https://doi.org/10.1016/S0921-5093\(99\)00662-0](https://doi.org/10.1016/S0921-5093(99)00662-0)
- [12] Paranthaman V, Dhinakaran V, Sai MS, Devaraju A. (2021) A systematic review of fatigue behaviour of laser welding titanium alloys. *Mater. Today: Proceedings* 2021;39: 520 – 523.  
<https://doi.org/10.1016/j.matpr.2020.08.249>
- [13] Chattopadhyay A, Muvvala G, Sarkar S, Racherla V, Nath AK. (2021) Effect of laser shock peening on microstructural, mechanical and corrosion properties of laser beam welded commercially pure titanium. *Opt Laser Technol* 2021;133: 106527.  
<https://doi.org/10.1016/j.optlastec.2020.106527>
- [14] Ao N, Liu D, Zhang X, Wu S. (2023) Improved fretting fatigue mechanism of surface-strengthened Ti-6Al-4V alloy induced by ultrasonic surface rolling process. *Int J Fatigue* 2023;170: 107567.  
<https://doi.org/10.1016/j.ijfatigue.2023.107567>
- [15] Ren ZY, Hu YL, Tong Y, et al. (2023) Wear-resistant NbMoTaWTi high entropy alloy coating prepared by laser cladding on TC4 titanium alloy. *Tribology International* 2023;182: 108366.  
<https://doi.org/10.1016/j.triboint.2023.108366>
- [16] Xu S, Cao Y, Duan B, Liu H, Wang J, Si C. (2023) Enhanced strength and sliding wear properties of gas nitrided Ti-6Al-4V alloy by ultrasonic shot peening pretreatment. *Surf. Coat. Technol* 2023;458: 129325.  
<https://doi.org/10.1016/j.surfcoat.2023.129325>
- [17] Wang Z, Zhou W, Luo K, Lu H, Lu J. (2023) Strengthening mechanism in thermomechanical fatigue properties of Ti6Al4V titanium alloy by laser shock peening. *Int J Fatigue* 2023;172: 107631.  
<https://doi.org/10.1016/j.ijfatigue.2023.107631>
- [18] Ren Z, Li Z, Zhou S, Wang Y, Zhang L, Zhang Z. (2022) Study on surface properties of Ti-6Al-4V titanium alloy by ultrasonic rolling. *Simul Model Pract Theory* 2022;121: 102643.  
<https://doi.org/10.1016/j.simpat.2022.102643>

- 
- [19] Qu S, Ren Z, Hu X, et al. (2021) The effect of electric pulse aided ultrasonic rolling processing on the microstructure evolution, surface properties, and fatigue properties of a titanium alloy Ti5Al4Mo6V2Nb1Fe. *Surf. Coat. Technol* 2021;421: 127408.  
<https://doi.org/10.1016/j.surfcoat.2021.127408>
- [20] Ao N, Liu D, Xu X, Zhang X, Liu D. (2019) Gradient nanostructure evolution and phase transformation of  $\alpha$  phase in Ti-6Al-4V alloy induced by ultrasonic surface rolling process. *Mater. Sci. Eng.: A* 2019;742: 820 – 834.  
<https://doi.org/10.1016/j.msea.2018.10.098>
- [21] Li ZM, Zhu YL, Du XK. (2013) The Anti-fatigue Mechanisms on Alterations of Structures and Performances of Alloy Welded Joints with Ultrasonic Impact Treatment. *Phys. Procedia* 50: 410–415.  
<https://doi.org/10.1016/j.phpro.2013.11.063>
- [22] Logesh M, Selvabharathi R, Thangeeswari T, Palani S. (2020) Influence of severe double shot peening on microstructure properties of Ti 6Al-4V and Titanium Grade 2 dissimilar joints using laser beam welding. *Optics & Laser Technol* 123: 105883.  
<https://doi.org/10.1016/j.optlastec.2019.105883>
- [23] Ren Z, Lai F, Qu S, Zhang Y, Li X, Yang C. (2020) Effect of ultrasonic surface rolling on surface layer properties and fretting wear properties of titanium alloy Ti5Al4Mo6V2Nb1Fe. *Surf. Coat. Technol* 389: 125612.  
<https://doi.org/10.1016/j.surfcoat.2020.125612>
- [24] Liu M, Li JY, Ma Y, Yuan TY, Mei QS. (2016) Surface nanocrystallization and property of Ti6Al4V alloy induced by high pressure surface rolling. *Surf. Coat. Technol* 289: 94–100.  
<https://doi.org/10.1016/j.surfcoat.2016.01.043>
- [25] Shi H, Liu D, Jia T, Zhang X, Zhao W. (2023) Effect of the ultrasonic surface rolling process and plasma electrolytic oxidation on the hot salt corrosion fatigue behavior of TC11 alloy. *International Journal of Fatigue* 168: 107443.  
<https://doi.org/10.1016/j.ijfatigue.2022.107443>
- [26] Liu C, Liu D, Zhang X, et al. (2019) On the influence of ultrasonic surface rolling process on surface integrity and fatigue performance of Ti-6Al-4V alloy. *Surf. Coat. Technol* 370: 24–34.  
<https://doi.org/10.1016/j.surfcoat.2019.04.080>
- [27] Pang Z, Wang S, Yin X, Yu S, Du N. (2022) Effect of spindle speed during ultrasonic rolling on surface integrity and fatigue performance of Ti6Al4V alloy. *Int J Fatigue* 159: 106794.  
<https://doi.org/10.1016/j.ijfatigue.2022.106794>
- [28] Luo X, Ren X, Qu H, Hou H, Chen J, Tian P. (2022) Research on influence of deep cryogenic treatment and ultrasonic rolling on improving surface integrity of Ti6Al4V alloy. *Mater. Sci. Eng.:*



A 843: 143142.

<https://doi.org/10.1016/j.msea.2022.143142>

[29] Zhao W, Liu D, Zhang X, et al. (2019) Improving the fretting and corrosion fatigue performance of 300M ultra-high strength steel using the ultrasonic surface rolling process. *Int J Fatigue* 121: 30–38.

<https://doi.org/10.1016/j.ijfatigue.2018.11.017>

[30] Wu D, Lv H, Wang H, Yu J. (2022) Surface micro-morphology and residual stress formation mechanisms of near-net-shaped blade produced by low-plasticity ultrasonic rolling strengthening process. *Mater. & Des.* 215: 110513.

<https://doi.org/10.1016/j.matdes.2022.110513>

[31] Wang F, Men X, Liu Y, Fu X. (2020) Experiment and simulation study on influence of ultrasonic rolling parameters on residual stress of Ti-6Al-4V alloy. *Simul Model Pract Theory* 104: 102121.

<https://doi.org/10.1016/j.simpat.2020.102121>

[32] Gedney BL, Rizos DC. (2022) Combining welding-induced residual stress with thermal and mechanical stress in continuous welded rail. *Results in Eng* 2022;16: 100777.

<https://doi.org/10.1016/j.rineng.2022.100777>

[33] Hobbacher AF. (2010) New developments at the recent update of the IIW recommendations for fatigue of welded joints and components. *Steel Constr* 3: 231–242.

<https://doi.org/10.1002/stco.201010030>

[34] Wang B, Cheng L, Li D. (2022) Study on very high cycle fatigue properties of forged TC4 titanium alloy treated by laser shock peening under three-point bending. *Int J Fatigue* 2022;156: 106668.

<https://doi.org/10.1016/j.ijfatigue.2021.106668>

[35] Luo X, Dang N, Wang X. (2021) The effect of laser shock peening, shot peening and their combination on the microstructure and fatigue properties of Ti-6Al-4V titanium alloy. *Int J Fatigue* 2021;153: 106465.

<https://doi.org/10.1016/j.ijfatigue.2021.106465>